

Experimental evaluation of noise equivalent passband, information capacity, and informational efficiency of yttrium based europium activated phosphors for use in x-ray imaging detectors*

D. Cavouras¹, I. Kandarakis¹, P. Prassopoulos², E. Kanellopoulos¹, C. D. Nomicos³ and G. S. Panayiotakis⁴

1. Department of Medical Instrumentation Technology, Technological Educational Institution of Athens, Ag. Spyridonos Street, Aigaleo, 122 10 Athens (Greece)

2. Department of Radiology, University Hospital, Medical School, University of Crete, Heraklion (Greece)

3. Department of Electronics, Technological Educational Institution of Athens, Ag. Spyridonos Street, Aigaleo, 122 10 Athens (Greece)

4. Department of Medical Physics, Medical School, University of Patras, 265 00 Patras (Greece)

Manuscript received: March 18, 1998; revised: June 26, 1998.

Accepted for publication: July 2, 1998.

Abstract

Three parameters expressing image quality by single indices, the noise equivalent passband, the information capacity, and the informational efficiency were studied. These indices were employed to assess the imaging performance of phosphor materials employed in detectors of x-ray imaging systems. The phosphors were in the form of screens prepared in laboratory from yttrium based europium activated materials emitting red light. The experimental determination of the three parameters was based on MTF, luminescence, and emission spectrum measurements. Results indicated that image information content decreases with screen coating weight and that among the three phosphors $Y_2O_3:Eu$ is the highest performing phosphor material.

KEY WORDS: x-ray luminescence; MTF; scintillators; image quality.

1. Introduction

The performance of imaging systems is often assessed by spatial frequency dependent parameters such as MTF, NPS, and DQE expressing contrast, spatial resolution, noise and signal to noise ratio. Image quality is, thus, described by means of curves giving the variation of the aforementioned quantities at a range of frequencies corresponding to the dimensions of objects to be imaged. However, it is often convenient to express the imaging performance of a system using only a single index, which may either be the value of the parameter at zero spatial frequency or its integral over the useful range of frequencies.

In the present study the following three indices, based on integration of spatial frequency dependent parameters, were studied in order to evaluate the performance of scintillators (phosphors) used in x-ray imaging detectors:

- i) The noise equivalent passband, expressing image sharpness [1].
- ii) The information capacity that quantifies the information contained in a diagnostic image by considering the number of discrete signal levels that can be registered on an image element [1-4].
- iii) The informational efficiency that compares the imaging performance of a real imaging system to the performance of a perfect system [3,4].

In evaluating these three indices, we have developed a method based on x-ray luminescence efficiency (XLE) and modulation transfer function (MTF) measurements. Each index was employed to assess the imaging performance of scintillators in the form of screens prepared in laboratory from yttrium based europium activated phosphors. These materials emit red light, which is very well detected [5,6] by red sensitive photographic emulsions and by the silicon photodiodes used in radiation detectors of digital imaging systems.

2. Materials and Methods

2.1. Noise equivalent passband.

The noise equivalent passband N_e , expressing image sharpness by a single number, has been defined [1] by the relation:

$$N_e = 2 \int_0^{\infty} MTF^2(\omega) d\omega \quad (1)$$

where, ω represents spatial frequency.

Relation (1) describes N_e as a quantity proportional to the area under the curve of the MTF squared graph.

*Author for correspondence: D. Cavouras, Ph.D., 37-39 Esperidon Street, Kallithea 17671, Athens, GREECE, e-mail: cavouras@hol.gr.; caovuras@ medisp.teiath.gr

2.2. Information capacity

It has been previously shown [1,3,4,7] that the information capacity (C_1) of an x-ray image receptor can be expressed as a function of the signal power spectrum (SPS) and the noise power spectrum (NPS) as follows:

$$C_1 = \pi \int_0^{\infty} \log_2 \left[1 + \frac{\text{SPS}(\omega)}{\text{NPS}(\omega)} \right] \omega d\omega \quad (2)$$

The functions SPS(ω) (see appendix A) and NPS(ω) [8] can be expressed in terms of the modulation transfer function (MTF(ω)) and parameters describing the processes of x-ray absorption, x-ray to light conversion, and light transmission and emission from an x-ray scintillation detector as:

$$\text{SPS}(\omega) = [Q\eta_Q(E, t)m_0(E, E_\lambda)G_L(\mu_0, t)\text{MTF}(\omega)]^2 \quad (3)$$

$$\text{NPS}(\omega) = Q\eta_Q(E, t)[m_0(E, E_\lambda)G_L(\mu_0, t)]^2 \text{MTF}^2(\omega) + Q\eta_Q(E, t)m_0(E, E_\lambda)G_L(\mu_0, t) \quad (4)$$

where, Q denotes the mean number of x-ray quanta incident on the detector area, η_Q is the x-ray quantum detection efficiency (QDE) expressing the probability of detection of an x-ray quantum, m_0 is the number of optical photons produced within the scintillator material after the detection of an x-ray quantum, G_L is the light transmission efficiency expressing the probability of an optical quantum to escape the scintillator. E_λ denotes the energy of one optical photon ($E_\lambda = hc/\lambda$), E is the energy of an x-ray quantum, μ_0 is the optical attenuation coefficient and t is the thickness of the scintillator. Q and m_0 are mean values of stochastic variables which were assumed to follow Poisson statistics [8]. η_Q and G_L express mean values – over image receptor area – of probabilities associated with binomial processes (e.g. x-ray detection or no detection, optical photon escape or no escape). MTF describes image contrast and spatial resolution degradation due to physical processes inducing lateral light spread due to isotropic emission and optical scattering.

The number m_0 of optical photons generated within the scintillator material can be calculated as:

$$m_0(E, E_\lambda) = \eta_c E / E_\lambda \quad (5)$$

where, η_c is the mean value of intrinsic x-ray to light conversion efficiency, giving the fraction of x-ray energy converted into light within the scintillator material. The product $\eta_Q\eta_cG_L$ is, by definition [9], equal to the x-ray luminescence efficiency (XLE) of a scintillator, giving the ratio of the light energy fluence emitted over the incident x-ray energy fluence. Thus, using relation (5) and the definition of XLE, the information capacity can be expressed as function of MTF and XLE:

$$C_1 = \pi \int_0^{\infty} \log_2 \left[1 + \frac{\eta_\phi(E, t)Q\epsilon(E, E_\lambda)\text{MTF}^2(\omega, t)}{\eta_c G(\mu_0, t)\epsilon(E, E_\lambda)\text{MTF}^2(\omega, t) + 1} \right] \omega d\omega \quad (6)$$

where,

$$\eta_\phi = \eta_c \eta_Q G_L, \quad \epsilon(E, E_\lambda) = E / E_\lambda$$

η_ϕ denotes the mean value of XLE. The values of parameters η_ϕ , ϵ , η_c , G , and MTF in (6) depend on intrinsic phosphor properties

2.3. Informational efficiency

The informational efficiency (η_I) has been defined [3,4] as:

$$\eta_I(E, t) = \frac{\text{DQE}(0) \text{Re}(E, t)}{\text{DQE}_{id}(0) \text{Re}(E, t)_{id}} \quad (7)$$

where, DQE(0) is the zero spatial frequency detective quantum efficiency, expressing the efficiency of an image receptor to transfer the SNR squared from the input to its output. The quantity Re has been defined [3,4] as:

$$\text{Re}(E, t) = \int_0^{\infty} \text{MTF}^2(\omega) \omega d\omega \quad (8)$$

Subscript id denotes that DQE(0) and Re correspond to an ideal imaging system. Since by definition $\text{DQE}_{id}(0)=1$ and $\text{MTF}(\omega)_{id}=1$, relation (7) reduces to

$$\eta_I(E, t) = \frac{\text{DQE}(0) \text{Re}(E, t)}{\int_0^{\infty} \omega d\omega} \quad (9)$$

DQE(0) can be expressed in terms of parameters η_Q , η_c , G_L describing the basic processes involved in an x-ray detection event (see appendix B) as:

$$\text{DQE}(0) = \frac{\eta_Q(E, t)\eta_c G_L(\mu_0, t)[E / E_\lambda]}{\eta_c G_L(\mu_0, t)[E / E_\lambda] + 1} \quad (10)$$

Using relations (7)-(10) and the definition of XLE, the informational efficiency can be written as:

$$\eta_I(E, t) = \left[\frac{\eta_\phi(E, t)[E / E_\lambda]}{\eta_c G_L(\mu_0, t)[E / E_\lambda] + 1} \right] \times \left[\frac{\int_0^{\infty} \text{MTF}^2(\omega) \omega d\omega}{\int_0^{\infty} \omega d\omega} \right] \quad (11)$$

2.4. Screen preparation

Scintillators were used in the form of fluorescent layers (screens). The screens were prepared from $Y_2O_2S:Eu$, $Y_2O_3:Eu$, and $YVO_4:Eu$ phosphor materials, which were supplied in powder form with mean grain size of about 7 μm . For screen preparation, a sedimentation technique was employed using 25ml of Na_2SiO_3 as binder material and 2000ml of de-ionized water. The coating weight of the screens ranged from approximately 20 mg/cm^2 to 150 mg/cm^2 .

2.5. MTF measurements

MTF was determined by the square wave response function (SWRF) method [6,10,11]. Screens were placed in contact with an Agfa Scopix LT2B film, which is very sensitive to the red light emitted by europium activated phosphors. To measure the SWRF, a resolution bar test pattern comprising line pairs with spatial frequencies from 0.25 to 10 lp/mm (Typ-53, Nuclear Associates Carle Place, N.Y.) was used. The pattern was placed in front of the phosphor screen area, which was irradiated using 80 kVp x-rays. The pattern image was formed on the film, which was placed in contact with the non irradiated back screen area. Images were digitized by a MICROTEC Scanner II SP (24-bit color, 1200x1200 dpi) CCD scanner. SWRF patterns were obtained by averaging 64 successive image traces perpendicularly directed with respect to the pattern line pairs. Data were corrected for screen-film non linearities by measuring the screen-film characteristic curve and converting image densities into exposure values [10]. MTF was finally computed using Coltman's formula:

$$MTF(\omega) = \frac{4}{\pi} \left[\frac{SWRF(\omega)}{\omega} + \frac{SWRF(3\omega)}{3\omega} - \frac{SWRF(5\omega)}{5\omega} + \dots \right] \quad (12)$$

In order to obtain the screen MTF, the MTF found in (12) was divided by the combined MTF of the acquisition system (radiographic film, CCD scanner). The combined MTF was determined by scanning the test pattern alone and considering the radiographic film MTF approximately equal to 1 for frequencies lower than 100 lp/cm [17].

2.6. X-ray luminescence measurements

The light energy fluence necessary to determine XLE was measured by exciting the screens using 80 kVp x-rays and employing an EMI 9558QB photomultiplier coupled to a Cary 401 vibrating reed electrometer [6,11-13]. X-ray exposure was measured at screen position by a PTW dosimeter. Exposure was converted into x-ray energy fluence and x-ray quantum flu-

ence employing the corresponding conversion factors [14]. X-ray energy fluence was employed in XLE determination while x-ray quantum fluence is the quantity Q in formulas (3), (4), (6).

In determining the light flux, a number of important parameters were taken into account: i/the geometric light collection efficiency between the phosphor screen and the photocathode of the photomultiplier, expressing the fraction of emitted screen light flux which is impinging on the photocathode's effective area. This efficiency depends on purely geometrical characteristics (e.g. distance between screen and photocathode, effective areas of screen and photocathode) and the angular distribution of the emitted light intensity, which was determined as described in previous studies [15]. ii/the spectral compatibility [5] between the phosphor's emission spectrum and the photocathode's (extended S-20) spectral sensitivity. The latter was obtained from manufacturer's data. The phosphors emission spectra were measured with an Oriel 7240 grating monochromator.

The product $\eta_c G_t$ in the denominator of the informational efficiency in relations (6) and (11) was calculated by dividing XLE by QDE (η_o/η_q). QDE was calculated considering exponential x-ray absorption within the phosphor material and using data on x-ray attenuation coefficients of the chemical elements as given by Storm and Israel [16]. It must be noted that E in relations (3)-(11) corresponds to the effective energy of the x-ray beam.

3. Results and Discussion

Figure 1 shows the MTFs of $Y_2O_2S:Eu$, $Y_2O_3:Eu$, and $YVO_4:Eu$ 80 mg/cm^2 phosphor screens, irradiated at 80 kVp. In Figure 2, the MTF at 20 lp/mm as function of screen coating weight is plotted. The MTF of $Y_2O_2S:Eu$ was found better than the MTF of $Y_2O_3:Eu$, which in turn was slightly higher than that of $YVO_4:Eu$. This MTF phosphor ranking is similar to an analogous phosphor ranking observed for XLEs in Figure 3. This is because the maximum optical density, depicting the spaces between pattern lines in the resulting SWRF image, is determined by the emitted intensity of light, which in turn is determined by the phosphor's XLE. Considering that the SWRF is related to the MTF as shown in relation (12), it is obvious that the MTF is affected by XLE. It must be noted, however, that high XLE values should be expected to widen the spatial distribution of output light, thus reducing MTF. Nevertheless, the importance of this effect is limited when comparing screens of equal coating weight but of different phosphor materials; $Y_2O_2S:Eu$ is denser than $Y_2O_3:Eu$ and the latter is denser than $YVO_4:Eu$. Screens of higher density are thinner than screens of equal coating weight but of lower density. Thus, lateral light spreading affecting spatial distribution is reduced in thin screens and this increases both output light intensity (XLE) and MTF. Our results on the MTF of europium activated phosphors

are comparable to published data [17] concerning commercial screen film systems.

Figure 4 shows the variation of the noise equivalent passband (Ne) with screen coating weight. Ne initially decreases with coating weight but shows a tendency to obtain a constant value at thick screens. This behaviour is due to the increasing effect of lateral light spread as screen thickness increases, which induces an image sharpness degradation. At thick screens, however, the lateral light trajectories are very

long causing a large fraction of the laterally directed photons to be absorbed before reaching the screen surface. Thus, at thick screens, the rate of sharpness degradation slows down and Ne attains approximately constant values. $Y_2O_2S:Eu$ gave better Ne values than $Y_2O_3:Eu$ which, in turn, was found better than $YVO_4:Eu$, as it was expected from the MTF data in Figure 1 and relation (1).

Figure 5 shows the results obtained for the information capacity of the three phosphors as function of

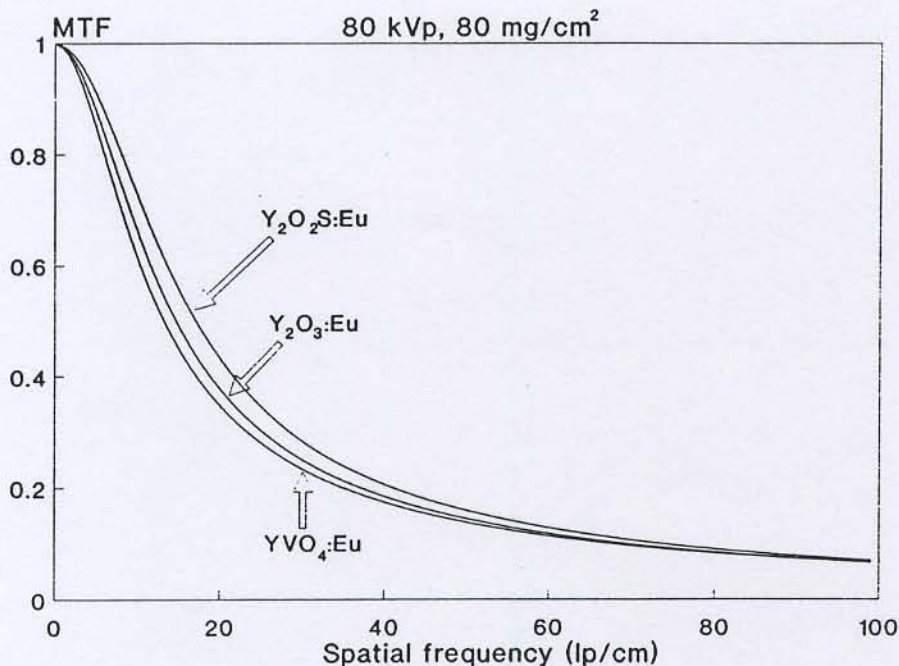


Fig. 1 – MTF curves of 80 mg/cm² $Y_2O_2S:Eu$, $Y_2O_3:Eu$, and $YVO_4:Eu$ phosphor screens.

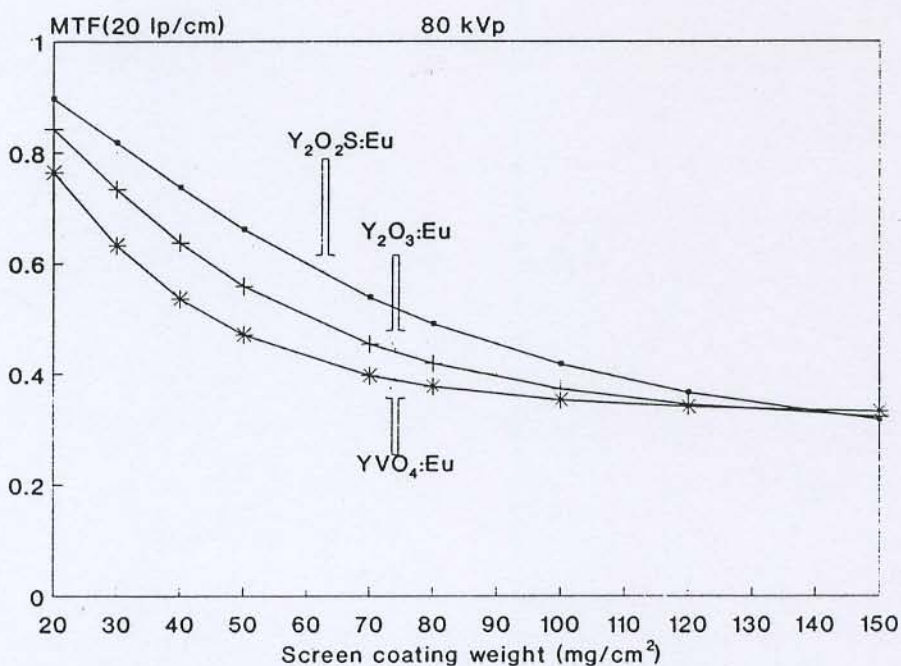


Fig. 2 – Variation of MTF (20 lp/cm) with screen coating weight.

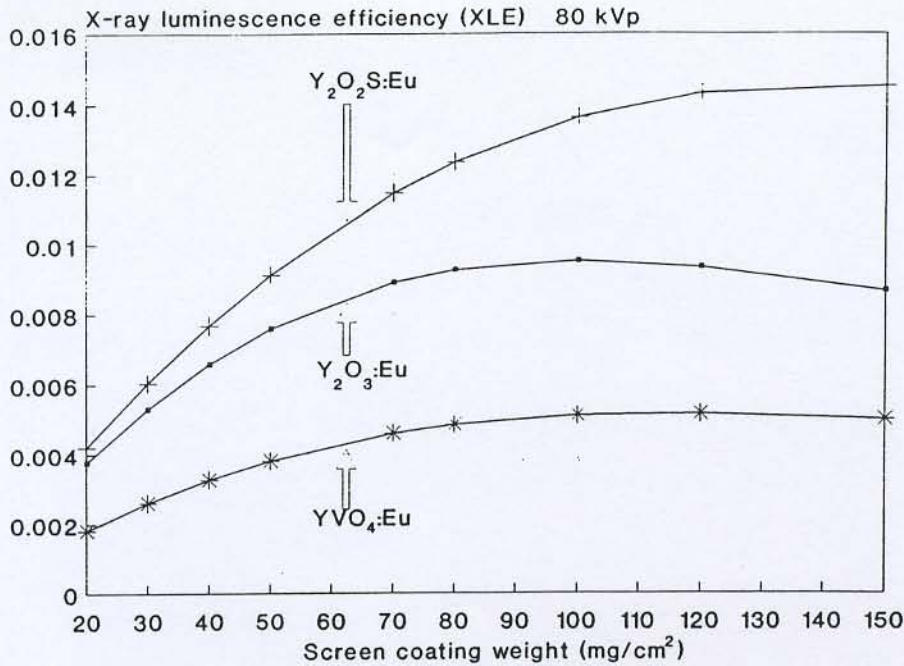


Fig. 3 - Variation of x-ray luminescence efficiency of Y₂O₂S:Eu, Y₂O₃:Eu, and YVO₄:Eu phosphor screens with screen coating weight.

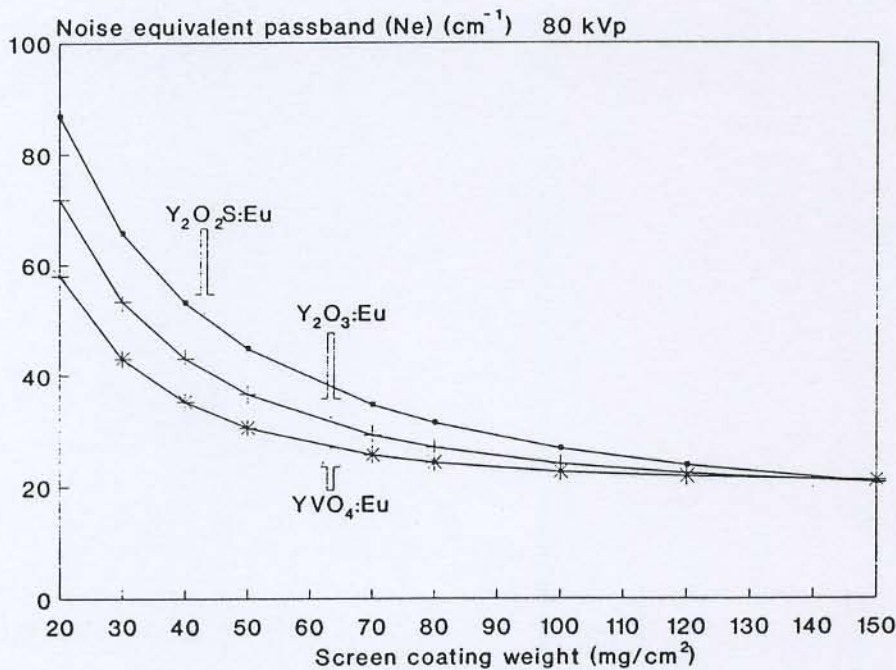


Fig. 4 - Variation of the noise equivalent passband of Y₂O₂S:Eu, Y₂O₃:Eu, and YVO₄:Eu phosphor screens with screen coating weight.

screen coating weight. Information capacity decreases with coating weight, being better for Y₂O₂S:Eu and lower for YVO₄:Eu. The results in Figure 5 are affected by the combined contributions of the corresponding XLEs and MTFs (see relation 6). MTF is decreasing with screen thickness (see Figure 2) while XLE varies slowly showing a tendency to saturate at high coating weights (see Figure 3). Thus, an optimal thickness for information capacity was not observed within the range of screen coating thicknesses considered in the present study. It is important to note

that although thick screens should absorb higher quantities of x-rays, the quantity of diagnostic information they can display in the finally produced image is lower as compared to the low coating weight screens. This effect can be explained by considering that in thick screens the light generated within the phosphor material is either attenuated during transmission through the thick phosphor layer similarly affecting XLE or is laterally spread inducing an image quality degradation as described by the results of noise equivalent passband. To compare our method on informa-

tion capacity with the findings of other workers, we have calculated the information spectrum of $Y_2O_2S:Eu$

using the term $\log_2 \left[1 + \frac{SPS(\omega)}{NPS(\omega)} \right]^{\frac{1}{2}}$ in equation (2) and

we have compared it with the only relevant published data on information capacity [7] known to us. Our results were approximately 30% higher which most probably is due to differences in exposure conditions and screen phosphor material.

Results concerning the informational efficiency are shown in Figure 6. The shape of the curves is similar to that concerning the information capacity in Figure 5. This indicates that for a specific phosphor material the information content in an x-ray image, as compared to an ideal imaging system, decreases with screen coating weight. This may be explained by following a similar reasoning as in the case of information capacity, since the informational efficiency depends on DQE, which is directly proportional to XLE in relations (10) and (11), and on MTF squared.

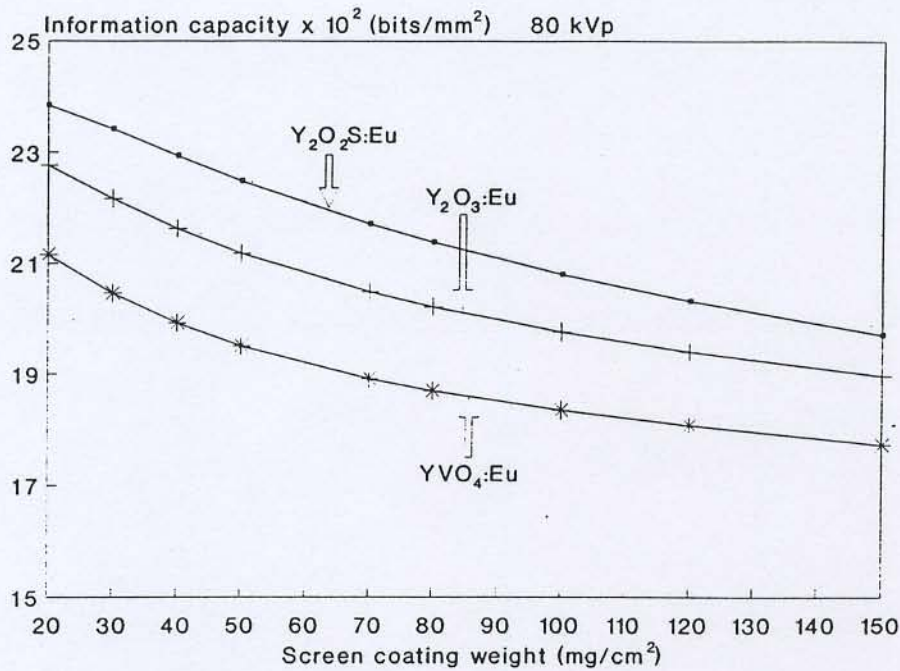


Fig. 5 – Variation of the information capacity of $Y_2O_2S:Eu$, $Y_2O_3:Eu$, and $YVO_4:Eu$ phosphor screens with screen coating weight.

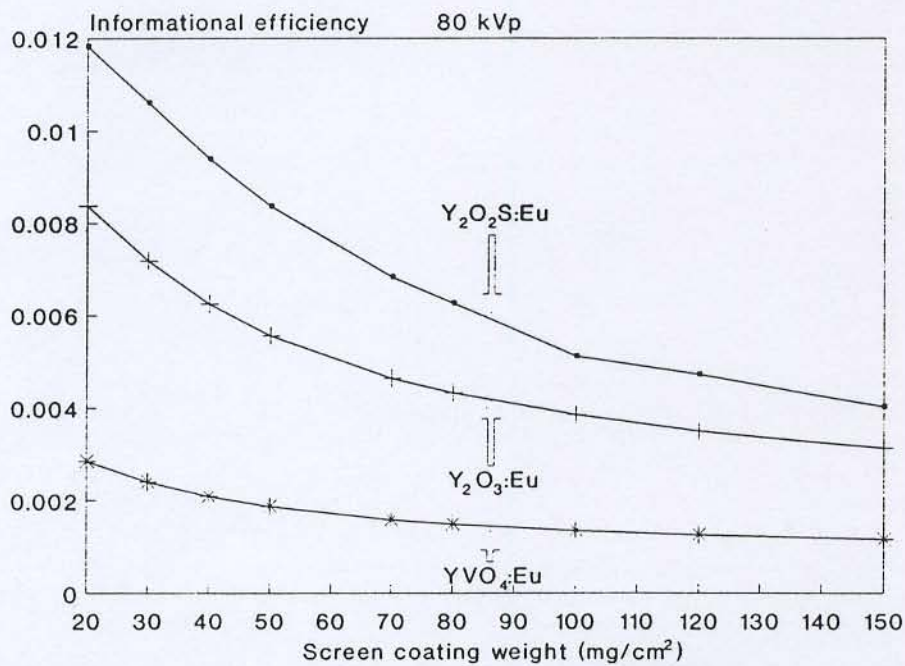


Fig. 6 – Variation of the informational efficiency of $Y_2O_2S:Eu$, $Y_2O_3:Eu$, and $YVO_4:Eu$ phosphor screens with screen coating weight.

Acknowledgment

This study is dedicated to the memory of Prof. G.E. Giakoumakis, leading member of our team, whose work on phosphor materials has inspired us to continue.

Appendix A

The signal spectrum can be evaluated by considering the following: Consider Q x-ray photons falling on the surface of the screen. A fraction of these photons are detected as determined by the quantum detection efficiency η_Q , giving the mean probability of x-ray detection over the screen area. A fraction η_c of the x-ray energy absorbed is converted into light energy. This energy is distributed in m_0 optical photons, which are transmitted to the screen output with a probability of transmission G_L (light transmission efficiency). These output optical photons consist the output signal of the screen and may be calculated as:

$$S_o = Q\eta_Q m_0 G_L = Q\eta_Q \eta_c [E/E_\lambda] G_L \quad (A1)$$

The output signal is distributed in the screen's rear surface according to the point spread function (PSF) of the screen. In the frequency domain, the PSF is represented by the modulation transfer function (MTF). This function is employed in normalized form as follows:

$$MTF(\omega, t) = \frac{S_o(\omega, t)}{S_o(0, t)} \quad (A2)$$

where, $S_o(\omega, t)$ is the frequency dependent output signal or signal spectrum and $S_o(0, t)$ is the zero frequency signal value evaluated in (A1). Thus, from (A1) and (A2) it follows that:

$$S_o(\omega, t) = [Q\eta_Q m_0 G_L] MTF(\omega, t) \quad (A3)$$

and for the signal power spectrum:

$$SPS(\omega, t) = [[Q\eta_Q \eta_c [E/E_\lambda] G_L] MTF(\omega, t)]^2 \quad (A4)$$

Appendix B

The detective quantum efficiency is defined by the ratio:

$$DQE = \left[\frac{SNR_o}{SNR_i} \right]^2 \quad (B1)$$

where, SNR_o and SNR_i are the output and input signal to noise ratios respectively. The zero spatial frequency output signal of an x-ray fluorescent screen may be expressed by the relation:

$$S_o(E, t) = Q\eta_Q \eta_c [E/E_\lambda] G_L \quad (B2)$$

where S_o is the mean value of the optical photons emitted. The signal to noise ratio is represented by the inverse square root of the relative variance in S_o , i.e. variance over mean value squared ($var(S_o)/S_o^2$). Q and $\eta_c(E/E_\lambda)$ were considered to follow Poisson statistics and, thus, the variances are equal to the mean values of Q and $\eta_c(E/E_\lambda)$. η_Q and G_L follow binomial processes and the corresponding variances are:

$$var(\eta_Q) = \eta_Q(1-\eta_Q) \quad (B3)$$

$$var(G_L) = G_L(1-G_L) \quad (B4)$$

The relative variance in S_o is given as the sum of the relative variances in Q , η_Q , $\eta_c(E/E_\lambda)$ and G_L . However, it must be taken into account that there will be Q events of the η_Q process, $Q\eta_Q$ events of $\eta_c(E/E_\lambda)$ and $Q\eta_Q \eta_c(E/E_\lambda)$ events of G_L . Thus, each relative variance must be multiplied by the inverse of the number of events. For instance, the term associated with the G_L process will be:

$$rel\ var(G_L)_M = \frac{1}{Q\eta_Q \eta_c(E/E_\lambda)} rel\ var(G_L)_S \quad (B5)$$

where, the relative variance with subscript M corresponds to multiple ($Q\eta_Q \eta_c(E/E_\lambda)$) events while the relative variance with S is associated with one single event. Thus,

$$rel\ val[S_o] = \frac{Q}{Q^2} + \frac{1}{Q} \cdot \frac{\eta_Q(1-\eta_Q)}{\eta_Q^2} + \frac{1}{\eta_Q Q} \cdot \frac{\eta_c(E/E_\lambda)}{[\eta_c(E/E_\lambda)]^2} + \frac{1}{\eta_Q Q \eta_c(E/E_\lambda)} \cdot \frac{G_L(1-G_L)}{G_L^2} \quad (B6)$$

From (B6) and considering that $SNR_o = [rel\ var(S_o)]^{-1/2}$ it follows that

$$SNR_o = \left[\frac{\eta_Q Q \eta_c(E/E_\lambda) G_L}{\eta_c(E/E_\lambda) G_L + 1} \right]^{1/2} \quad (B7)$$

The input signal to noise ratio may be written as the inverse square root of the relative variance in Q . Thus,

$$rel\ var(Q) = \frac{Q}{Q^2} \quad (B8)$$

and

$$SNR_i = [rel\ var(Q)]^{-1/2} = Q^{1/2} \quad (B9)$$

From (B7) and (B9) it follows that

$$DQE = \frac{\eta_Q \eta_c(E/E_\lambda) G_L}{\eta_c(E/E_\lambda) G_L + 1} \quad (B10)$$

REFERENCES

- [1] Evans AL. The evaluation of medical images. Bristol. Adam Hilger Ltd 1981; 45-46.
- [2] Shannon CE. A mathematical theory of communication. *Bell. Syst. Tech. J.* 1993; 27; 379-623.
- [3] Dainty JC and Shaw R. Detective quantum efficiency, signal to noise ratio, and the noise equivalent number of quanta. In: *Image science*. New York. Academic Press 1974; 152-88.
- [4] Shaw R. *The Physics of Medical Imaging: Recording System, Measurements and Techniques*. New York. American Association of Physicists in Medicine 1979; 515-23.
- [5] Panayiotakis G, Cavouras D, Kandarakis I, Nomicos C. A study of X-ray luminescence and spectral compatibility of europium-activated yttrium-vanadate (YVO₄:Eu) screens for medical imaging applications *Appl. Phys. A* 1996; 62; 483-6.
- [6] Cavouras D, Kandarakis I, Panayiotakis G, Evangelou EK, Nomicos CD. An evaluation of the Y₂O₃:Eu³⁺ scintillator for application in medical x-ray detectors and image receptors. *Med. Phys.* 1996; 23; 1965-75.
- [7] Kanamori H and Matsuoto M. The information spectrum as a measure of radiographic image quality and system performance. *Phys. Med. Biol* 1984; 29; 303-13.
- [8] Shaw R and Van Metter R. An analysis of the fundamental limitations of screen-film systems for x-ray detection. *Proc. SPIE* 1984; 454; 128-32.
- [9] Ludwig GW. X-ray efficiency of powder phosphors. *J. Electrochem. Soc.* 1971; 118; 1152-9.
- [10] Barnes GT. The use of bar pattern test objects in assessing the resolution of film/screen systems. In: *The Physics of Medical Imaging Recording System Measurements and Techniques*. Haus AG Ed. New York. American Association of Physicists in Medicine 1979; 138-51.
- [11] Kandarakis I, Cavouras D, Panayiotakis G, Agelis T, Nomicos C, Giakoumakis G. X-ray induced luminescence and spatial resolution of La₂O₃S:Tb phosphor screens. *Phys. Med. Biol.* 1996; 41; 297-307.
- [12] Kandarakis I, Cavouras D, Panayiotakis GS, and Nomicos C. Evaluating x-ray detectors for radiographic applications: a comparison of ZnSCdS:Ag with Gd₂O₃S:Tb and Y₂O₃S:Tb screens. *Phys Med Biol* 1997; 42; 1351-73.
- [13] Kandarakis I, Cavouras D, Panayiotakis GS, Triantis D, and Nomicos CD. An experimental method for the determination of spatial frequency dependent detective quantum efficiency (DQE) of scintillators used in x-ray imaging detectors. *Nucl. Instr. and Meth. Phys. Res. A* 1997; 399; 335-342.
- [14] Hendee WR. *Medical Radiation Physics*. Chicago. Year Book Medical Publishers, 1970; 145-8.
- [15] Giakoumakis GE and Miliotis DM. Light angular distribution of fluorescent screens excited by x-rays. *Phys. Med. Biol.* 1985; 30; 21-9
- [16] Storm E and Israel H. Photon cross-sections from 0.001 to 100 MeV for elements 1 through 100. Report LA-3753, Los Alamos Scientific Laboratory, University of California 1967.
- [17] Beutel J, Mickewich D J, Issler SL and Shaw R. The image quality characteristics of a novel ultra-high-resolution film/screen system. *Phys. Med. Biol.* 1993; 38; 1195-1206.